Inter-laboratory comparison between NMIJ and KRISS of calibration capabilities for torque measuring devices in the range from 50 N·m to 2 kN·m

Koji Ogushi[1], Atsuhiro Nishino[1], Kazunaga Ueda[1], Min-Seok Kim[2] and Yon-Kyu Park[2]

[1]*National Metrology Institute of Japan, AIST, Tsukuba Central 3, 1-1-1 Umezono, Tsukuba, Ibaraki, 305-8563, Japan*
[2]*Korea Research Institute of Standards and Science, 267 Gajeong-Ro, Yuseong-Gu, Daejeon, 305-340, Rep. of Korea*

ABSTRACT
An inter-laboratory comparison of the calibration capability for torque measuring devices (TMDs) was conducted between the National Metrology Institute of Japan (NMIJ) in the National Institute of Advanced Industrial Science and Technology (AIST) and the Korea Research Institute of Standards and Science (KRISS). Three high-performance torque transducers having rated capacities of 100 N·m, 1 kN·m, and 2 kN·m, and a bridge calibration unit (BN100A) were used as the transfer devices. The 1 kN·m and 2 kN·m transducers had one bridge, but the 100 N·m transducer had two bridges that acquired data more reliably. An identical indicator/amplifier type (DMP40) owned by each laboratory was used. All of the transducers and BN100A were transferred from NMIJ to KRISS. For the comparison, NMIJ used 1 kN·m and 20 kN·m deadweight torque standard machines (TSMs), and KRISS used a 2 kN·m deadweight TSM. In particular, the capability of the 1 kN·m TSM at NMIJ was examined after some improvements. In the calibration range from 50 N·m to 2 kN·m, relative deviations were less than 3.0×10^{-5} for increasing torques. Sufficiently small deviations were obtained between the calibration results in the two laboratories, as compared with their calibration and measurement capabilities (CMCs), which were 3.5×10^{-5} for the 1 kN·m TSM at NMIJ, 7.0×10^{-5} for the 20 kN·m TSM at NMIJ, and 5.0×10^{-5} for the 2 kN·m TSM at KRISS (as relative expanded uncertainties).

Corresponding author: Koji Ogushi, e-mail: kji.ogushi@aist.go.jp

1. INTRODUCTION

Torque standard machines (TSMs) in national metrology institutes (NMIs) have been established in many countries over the last two decades. The Korea Research Institute of Standards and Science (KRISS) has developed two deadweight-type TSMs (DWTSMs), which have rated capacities of 100 N·m and 2 kN·m (100-N·m-DWTSM(K) and 2-kN·m-DWTSM(K), respectively) [1]. A new deadweight-type TSM with a rated capacity of 20 kN·m (20-kN·m-DWTSM(K)) is also being developed [2]. The National Metrology Institute of Japan (NMIJ) has also developed three DWTSMs, which have rated capacities of 10 N·m (10-N·m-DWTSM(J)) [3], 1 kN·m (1-kN·m-DWTSM(J)) [4], and 20 kN·m (20-kN·m-DWTSM(J)) [5].

The first bilateral comparison between NMIJ and KRISS was performed in 2004 for the range from 200 N·m to 2 kN·m by using 1-kN·m-DWTSM(J) and 20-kN·m-DWTSM(J) at NMIJ and 2-kN·m-DWTSM(K) at KRISS [6]. After that, 1-kN·m-DWTSM(J) was improved to reduce the relative expanded uncertainty (REU) of the realized torque [7]. In order to confirm this improvement and to confirm the stability of other TSMs after the first comparison, a second bilateral comparison between NMIJ and KRISS was conducted in 2010 for the range from 50 N·m to 2 kN·m. Although the evaluation was put on hold after the Great East Japan Earthquake on March 11, 2011, the evaluation was resumed in 2014. This paper describes the second comparison results. We also investigated the influence

of the voltage span of the indicator/amplifiers by using a bridge calibration unit as well as the temperature and humidity coefficients of the transducers.

2. TORQUE STANDARD MACHINES

2.1. NMIJ/AIST

Two deadweight machines, 1-kN·m-DWTSM(J) and 20-kN·m-DWTSM(J), were used for the comparison at NMIJ. Figure 1 shows 1-kN·m-DWTSM, which has a calibration range from 5 N·m to 1 kN·m. The lower limit of the range was extended to 0.5 N·m by developing a new small linkage series of weights; 1-kN·m-DWTSM(J) was also improved to reduce the uncertainty of the moment arm length by changing the metal band thickness at the end of the arm from 100 μm to 50 μm and re-evaluating the sensitivity limit of the fulcrum (aerostatic bearing). As a result of these evaluations, REUs ($k = 2$) of 7.3×10^{-5} and 2.9×10^{-5} could be obtained for the ranges from 0.5 N·m to 20 N·m and from 5 N·m to 1 kN·m, respectively [7]. After some other minor changes, such as the environmental conditions, an REU of 3.4×10^{-5} for the realized torque was obtained in the range from 5 N·m to 1 kN·m.

Figure 2 shows 20-kN·m-DWTSM(J), which has a calibration range from 200 N·m to 20 kN·m. The REU of the torque realized with the TSM was 6.7×10^{-5} [5]. The calibration and measurement capabilities (CMCs), which equal the REUs ($k = 2$) of the calibration with almost ideal torque measuring devices (TMDs), were 3.5×10^{-5} for 1-kN·m-DWTSM(J) from 5 N·m to 1 kN·m and 7.0×10^{-5} for 20-kN·m-DWTSM(J).
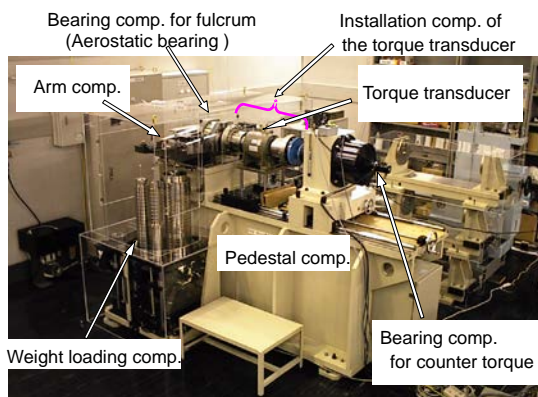
Figure 1. Components of 1-kN·m-DWTSM at NMIJ.
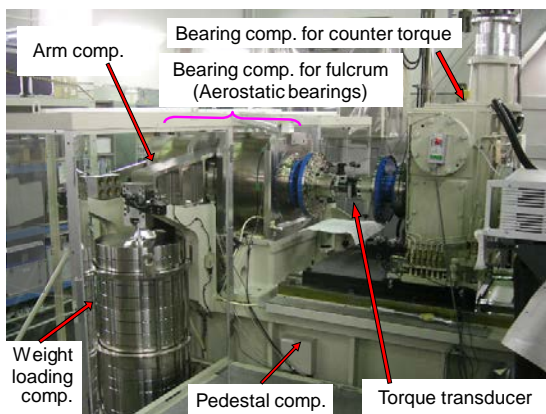
Figure 2. Components of 20-kN·m-DWTSM at NMIJ.

2.2. KRISS

The 2-kN·m-DWTSM(K) deadweight machine was used for the comparison at KRISS. The CMC of 2-kN·m-DWTSM was evaluated as 5.0×10^{-5} [1]. Figure 3 shows 2-kN·m-DWTSM(K). The characteristics of 2-kN·m-DWTSM can be found in references [1] and [6].

3. TRANSFER DEVICES

3.1. Torque transducers

Three torque transducers of different capacities were used as the transfer devices for this comparison. The three transducers, which have rated capacities of 2 kN·m (TN/2kNm), 1 kN·m (TB2/1kNm), and 100 N·m (TN/100Nm), were transferred from NMIJ to KRISS by air transport. Figures 4 and 5 show
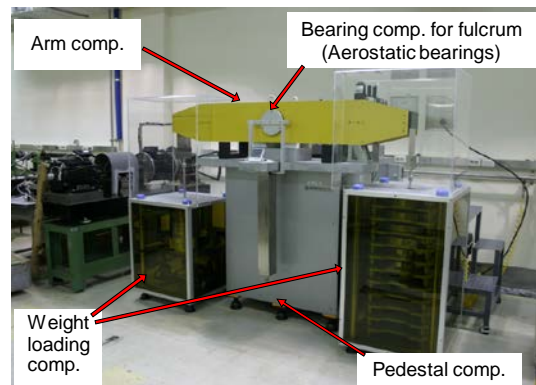
Figure 3. Components of 2-kN·m-DWTSM at KRISS.
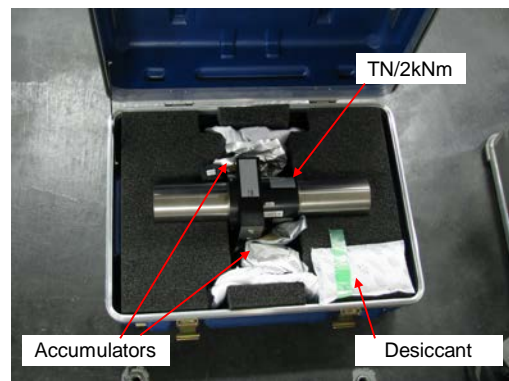
Figure 4. 2 kN·m transducer and its container.
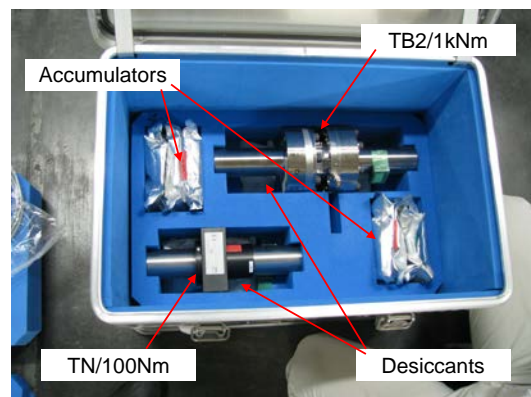
Figure 5. 1 kN·m and 100 N·m transducers and their container.

the transducers and their special containers. TN/2kNm and TN/100Nm are shaft-type transducers, whereas TB2/1kNm is a disk-type transducer. The adapter flanges were kept fastened to both sides of TB2/1kNm for more than one year before the comparison. The 100 N·m transducer of TN/100Nm has double bridges so that two series of outputs were available. The output from bridge 1 is expressed as TN/100Nm(MD1), whereas that of bridge 2 is expressed as TN/100Nm(MD2). The containers sealed the transducers from the outside environment. Accumulators (20 °C to 25 °C) and desiccants (40 % relative humidity) were put into the containers to maintain the lab environment as much as possible. Thermo-hygrometers and a 3-D accelerometer were placed in the container to monitor the environmental conditions. The sampling period of the thermo-hygrometers was 30 minutes. The variations in temperature and relative humidity during transportation were from 10 °C to 24 °C and from 28 % to 63 %, respectively. The sampling period of the accelerometer was 0.5 s, and the maximum acceleration was recorded for every hour. The containers inadvertently received a maximum shock of 76 m/s² (one time) during transportation. However, no serious damage was found in the transducer after unpacking.

Figures 6(a)–6(d) indicate the long-term stabilities of TN/2kNm, TB2/1kNm, and TN/100Nm(MD1 and MD2) before the comparison. The long-term stability was expressed by relative deviations of the calibration results at the rated capacities from the mean values of all calibration results during a certain period. TN/2kNm and both bridges of TN/100Nm were stable, and the maximum variation over approximately three months was less than 1.0×10^{-5}. The variation of

TB2/1kNm over approximately one and half years was 7.0×10^{-5}. Although the variation was relatively large, the tendency of the variation was approximately linear, and the change in calibration results within three months was less than 2.0×10^{-5}, so the authors decided that the transducer could be used as a transfer standard.

The temperature and humidity coefficients of all transducers were investigated after the comparison in order to correct the results depending on the environmental conditions during each measurement. The detailed procedure and results are explained and discussed in Sections 4.2 and 5.3.

3.2. Amplifier/indicators and bridge calibration unit

The bridge calibration unit BN100A(J), which calibrates the AC bridge voltage with an excitation voltage of 5 V and a carrier frequency of 225 Hz, was also transferred from NMIJ to KRISS by air transport. The amplifier/indicator of each NMI (DMP40S2(J_a) and DMP40S2(J_b) at NMIJ and DMP40(K) at KRISS) was connected to the transfer transducers during each torque calibration. At NMIJ, DMP40S2(J_a) was used for the calibrations of TB2/1kNm and TN/100Nm, whereas DMP40S2(J_b) was used for the calibrations of TN/2kNm. At KRISS, DMP40(K) was used for the calibrations of all transducers. The amplifier/indicators were calibrated just before and immediately after each torque calibration by BN100A(J). Figure 7 shows BN100A(J) and DMP40(K). The reference voltage ratios of the bridge calibration unit were measured by the amplifier/indicators at steps of +0, +0.1, +0.5, +0.7, +0.8, +1.0, +1.4, and +1.6 mV/V and then -0, -0.1, -0.5, -0.7, -0.8, -1.0, -1.4, and -1.6 mV/V. Bridge voltage calibration was carried out 10 times during this comparison calibration, as

(a) TN/2kNm

(b) TB2/1kNm

(c) TN/100Nm(MD1)

(d) TN/100Nm(MD2)
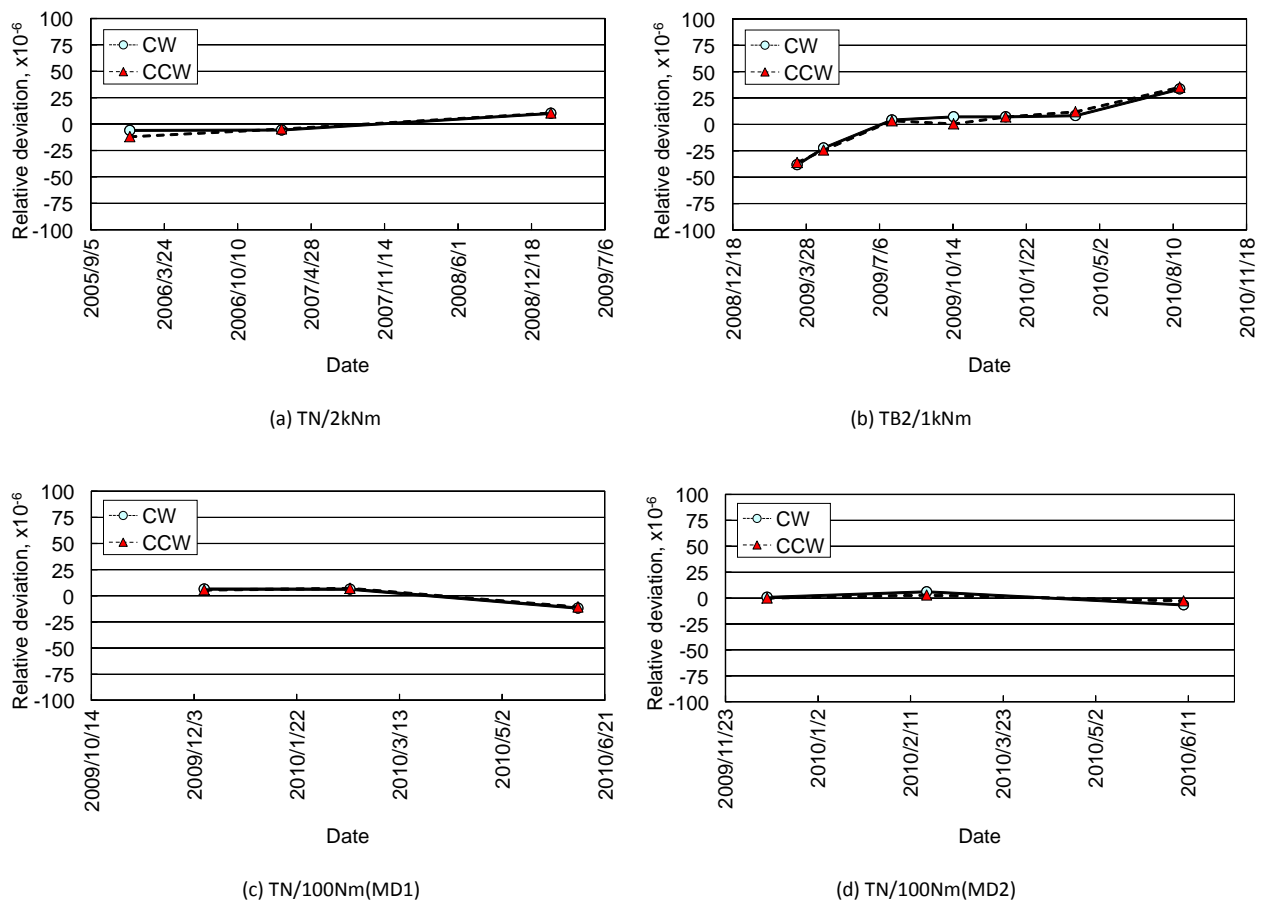
Figure 6. Long-term stabilities of the torque transducers.
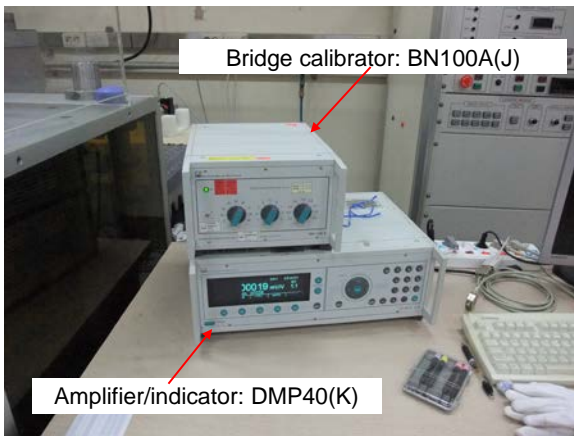
Figure 7. Bridge calibration unit and amplifier/indicator.

follows:

(V1) DMP40S2(J_a) calibrated by BN100A(J) before pre-cal. at NMIJ
(V2) DMP40S2(J_a) calibrated by BN100A(J) after pre-cal. at NMIJ
(V3) DMP40S2(J_b) calibrated by BN100A(J) before pre-cal. at NMIJ
(V4) DMP40S2(J_b) calibrated by BN100A(J) after pre-cal. at NMIJ
(V5) DMP40(K) calibrated by BN100A(J) before calibration at KRISS
(V6) DMP40(K) calibrated by BN100A(J) after calibration at KRISS
(V7) DMP40S2(J_a) calibrated by BN100A(J) before post-cal. at NMIJ
(V8) DMP40S2(J_a) calibrated by BN100A(J) after post-cal. at NMIJ
(V9) DMP40S2(J_b) calibrated by BN100A(J) before post-cal. at NMIJ
(V10) DMP40S2(J_b) calibrated by BN100A(J) after post-cal. at NMIJ

The above procedure was able to evaluate the stability and differences of amplifier/indicators during the entire comparison calibration. Results are discussed in Section 5.1.

4. EXPERIMENTAL PROCEDURE

4.1. Comparison calibration procedure

Pre- and post-calibrations were conducted at NMIJ (we call the pre-calibration "J1" and the post-calibration "J2") by three transducers (four bridges) before and after the calibration at KRISS (we call the calibration "K"). Loading timetables for the individual calibrations are shown in Figure 8. The timetable used in the CIPM key comparison of CCM.T-K2 [8] was adopted. The torque calibration was conducted separately in both the clockwise (CW) and counterclockwise (CCW)
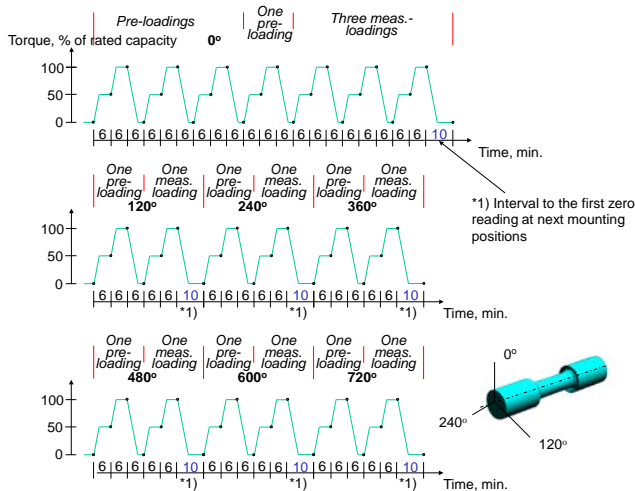
Figure 8. Loading timetable of calibration for each torque transducer.

directions. Table 1 shows the overall schedule of the comparison.

The rotational mounting position of each transducer was changed to three pitch directions (every 120°) and rotated twice. First, after three pre-loading cycles up to the maximum torque (the rated capacity of the torque transducer) in two steps of 50 % and 100 % of the maximum torque, the combination of one pre-loading and three measurement loading cycles was conducted at the 0° direction. In all cycles, the torque steps were increasing only. The combination of one pre-loading and one measurement loading cycle was performed in the directions of 120°, 240°, 360°, 480°, 600°, and 720°. The time intervals were strictly maintained to exclude the influence of the creep characteristics of transducers. The interval from the start of loading to data acquisition was six minutes. The interval from the last maximum torque reading at the present mounting position to the first zero reading at the next mounting position was ten minutes.

4.2. Determination procedure of temperature and humidity coefficients

The principle of measurement for the torque transducers used in this comparison was the strain gauge. The output of this type of transducer generally depends on the environmental temperature and humidity [9]. After the comparison calibration, therefore, temperature and humidity coefficients were experimentally determined. We prepared the following five conditions in the torque calibration rooms at NMIJ, and torque was loaded on the transducers in steps of 50 % and 100 % of the maximum torque, as was done in the comparison calibration procedure (but with only three pre-loading cycles and one measurement loading cycle at only the 0° position, and the time interval was approximately 40 seconds, but not six minutes).

DATA 1: 23 °C, 40 %
DATA 2: 25 °C, 40 %
DATA 3: 27 °C, 40 %
DATA 4: 27 °C, 50 %
DATA 5: 27 °C, 60 %

From the measurement values of the five conditions, temperature coefficient α_t and humidity coefficient β_h were estimated for both the 50 % and 100 % steps and for both the CW and CCW directions of all bridges.

5. RESULTS AND DISCUSSION

5.1. Stability and differences of amplifier/indicators

All measurement results are summarized in Figures 9(a) and 9(b), where the relative deviation of each step from the start of measurement is expressed. Figures 9(a) and 9(b) are the cases referring to DMP40S2(J_a) and DMP40S2(J_b), respectively. In both cases, very small voltage span variations occurred except at the steps of ± 0.1 mV/V. From the differences of voltage

Table 1. Schedule of measurements and transportation.

Pre-calibration at NMIJ (J1)	September 13 – September 24, 2010
Transportation	September 24 – October 5, 2010
Calibration at KRISS (K)	October 5 – October 21, 2010
Transportation	October 26 – October 29, 2010
Post-calibration at NMIJ (J2)	November 1 – December 2, 2010

(a) Referring to DMP40S2(J$_a$)

(b) Referring to DMP40S2(J$_b$)
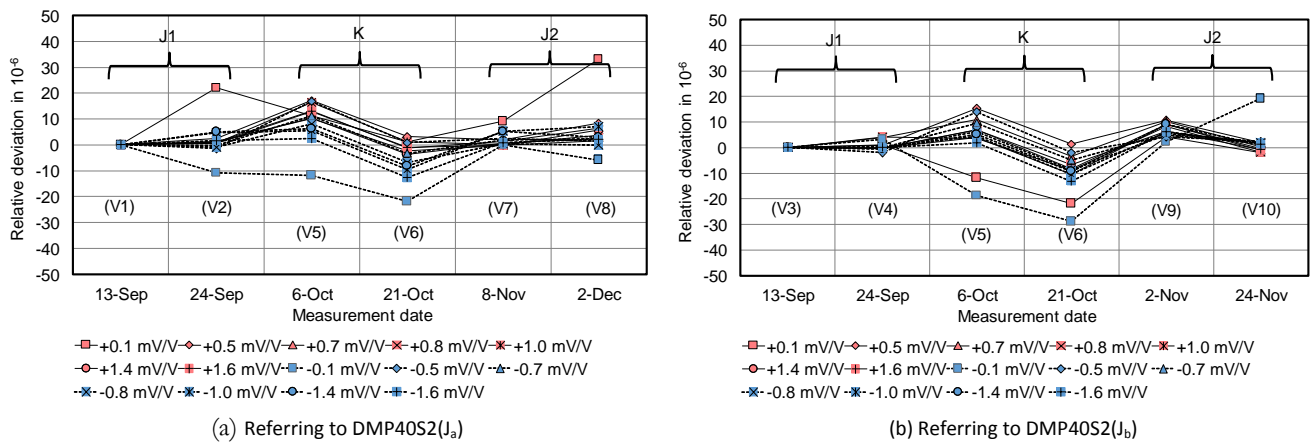
Figure 9. Stability and differences of voltage span in amplifier/indicators.

ratios between DMP40s in NMIJ and KRISS, we calculated correction factors and uncertainties for the torque calibration values obtained in KRISS according to the procedure in reference [6], as shown in Table 2. The correction factors are so small that they would not affect the final results of the comparison. Nevertheless, these factors were used for the correction of the results in Sections 5.3 and 5.4.

5.2. Calibration results of torque without correction

The calibration results were calculated by using the following equation for the mean of the measured values which are defined as each indicated value minus the zero value at the prior loading cycle, at the measurement loading cycles for all mounting positions except the 0° direction:

$$\overline{S'_i} = \frac{1}{n_{rot}} \sum_{e=1}^{n_{rot}} S'_{i1e} \qquad (1)$$

where S'_{ije} is the measured value in the measurement loading cycle for step i, cycle j (=1), and series e (where "series" means the successive calibration sequence within the same mounting position), and n_{rot} is the number of rotational mounting positions ($n_{rot} = 6$). The relative deviations of the calibration results obtained at KRISS from the mean results of the pre- and post-calibrations at NMIJ are shown in Figures 10(a)–10(d) (with white squares) for TN/2kNm, TB2/1kNm, TN/100Nm(MD1), and TN/100Nm(MD2), respectively. The

short-term drift, which is expressed by (11) in Section 5.4.5, is defined as the difference in the results between the pre- and post-calibrations at NMIJ. The relative values of the short-term drift are also shown in Figure 10 (with white circles).

At the calibration points for 2 kN·m, 1 kN·m, 500 N·m, 100 N·m, and 50 N·m, the relative deviations were from 0.2×10^{-5} to 5.0×10^{-5}. At some points, very small deviations were obtained, whereas relatively large deviations occurred in the 50 N·m and 100 N·m steps. The deviation tendency in TN/100Nm(MD1) was similar to that in TN/100Nm(MD2). The deviation of TN/2kNm in the CW direction became larger than the others. The authors presume that the differences in such deviation levels are due to the differences in environmental conditions, humidity in particular. The environmental conditions during each torque calibration are summarized in Table 3. Some of the short-term drifts of the transducers for approximately two months were also larger than the others (0.3×10^{-5} to 3.8×10^{-5}).

5.3. Determination of temperature and humidity coefficients

Figure 11 shows the actual temperature and relative humidity measured at each condition and for each transducer (as described in Section 4.2). Because the torque calibration rooms are very huge, the temperature and humidity are very stable, but it was difficult to precisely set the temperature and humidity to objective values. The dispersions and deviations occurred even

Table 2. Correction factors due to differences of voltage ratios.

Transducer	Torque steps in N·m	Equivalent voltage ratio steps in mV/V	Correction factor for KRISS values	Relative standard uncertainty
TN/2kNm	1000	+0.7 to +0.8	1.000003	1.2.E-05
	2000	+1.4 to +1.6	1.000003	1.2.E-05
	-1000	-0.7 to -0.8	1.000000	1.1.E-05
	-2000	-1.4 to -1.6	1.000005	1.1.E-05
TB2/1kNm	500	+0.5	0.999993	1.1.E-05
	1000	+1.0	0.999992	1.1.E-05
	-500	-0.5	0.999992	1.2.E-05
	-1000	-1.0	1.000006	1.1.E-05
TN/100Nm(MD1)	50	+0.7 to +0.8	0.999997	1.1.E-05
	100	+1.4 to +1.6	0.999996	1.1.E-05
	-50	-0.7 to -0.8	0.999998	1.0.E-05
	-100	-1.4 to -1.6	1.000005	1.0.E-05
TN/100Nm(MD2)	50	+0.7 to +0.8	0.999997	1.1.E-05
	100	+1.4 to +1.6	0.999996	1.1.E-05
	-50	-0.7 to -0.8	0.999998	1.0.E-05
	-100	-1.4 to -1.6	1.000005	1.0.E-05
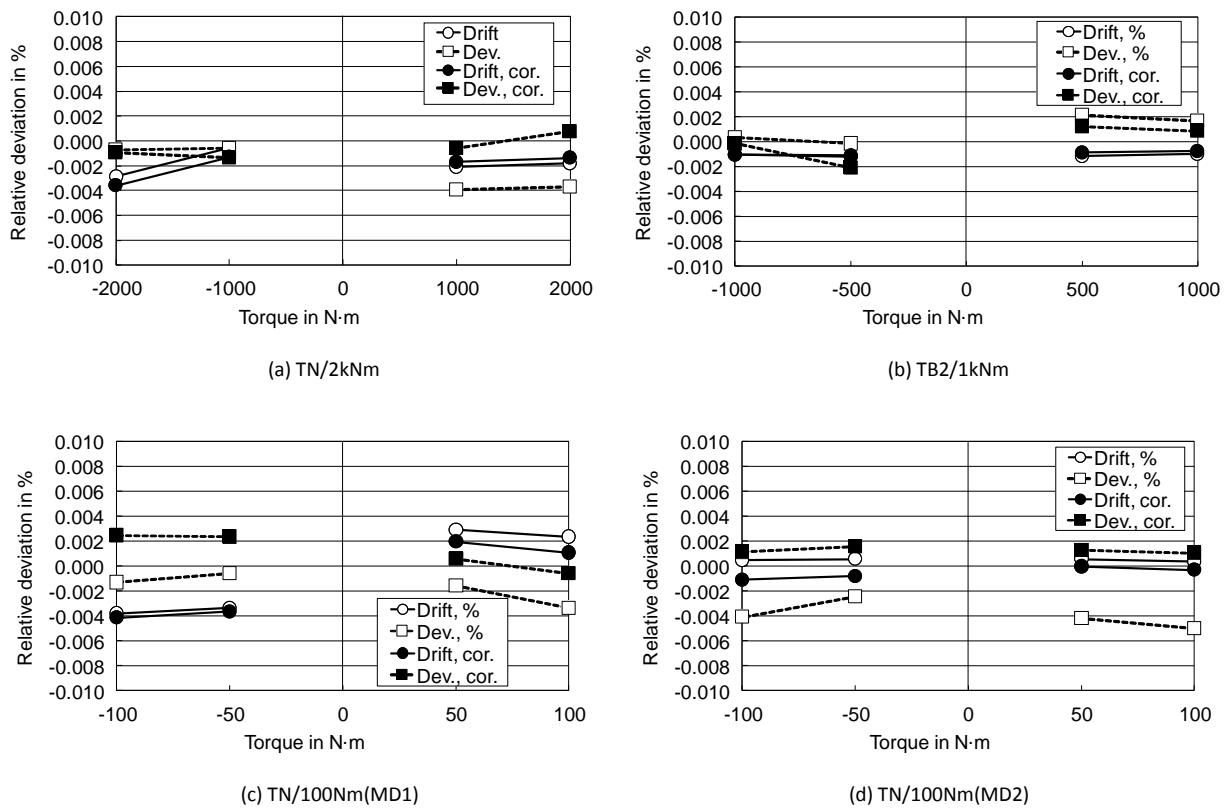
Figure 10. Relative deviation and short-term drift of calibration results.

Table 3. Temperature and humidity conditions at each measurement.

			J1 Temp. in °C	J1 R. H. in %	K Temp. in °C	K R. H. in %	J2 Temp. in °C	J2 R. H. in %
TN/2kNm								
CW	Min.		22.9	36	23.1	49	22.8	37
	Max.		23.1	37	23.5	53	22.9	39
CCW	Min.		22.7	37	23.3	36	22.9	37
	Max.		22.9	45	23.5	42	23.0	39
TB2/1kNm								
CW	Min.		23.1	41	23.3	47	22.7	39
	Max.		23.3	42	23.6	50	23.0	40
CCW	Min.		23.2	40	23.4	48	22.8	40
	Max.		23.3	40	23.6	51	23.0	44
TN/100Nm(MD1)								
CW	Min.		23.1	40	22.6	50	22.8	39
	Max.		23.2	47	22.9	53	22.9	40
CCW	Min.		23.0	42	23.0	52	22.8	40
	Max.		22.9	39	22.9	51	22.7	40
TN/100Nm(MD2)								
CW	Min.		23.1	40	22.6	50	22.8	39
	Max.		23.2	47	22.9	53	22.9	40
CCW	Min.		23.0	42	23.0	52	22.8	40
	Max.		23.0	42	23.0	52	22.8	40

under the same conditions.

Nevertheless, DATA 3, 4, and 5 have comparably similar temperature values (around 27.3 °C). So, we decided to carry out the following procedures:

(1) Humidity coefficient β_h for each transducer, each direction and each step was estimated by fitting the linear curve

for three measurement results of DATA 3, 4, and 5.

(2) Measurement values of DATA 1 and 2 were corrected to values at the humidity of DATA 3 by using the humidity coefficient obtained by procedure (1).

(3) Corrected measurement values of DATA 1, 2, and 3 have the same humidity conditions and different temperature
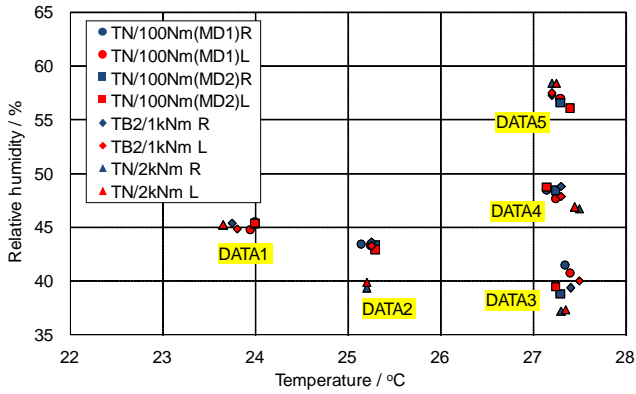
Figure 11. Actual temperature and relative humidity at each experimental condition to determine the temperature and humidity coefficients of the torque transducers.

conditions. Then, temperature coefficient α_t for each transducer, each direction and each step was estimated by fitting the linear curve for three corrected measurement results of DATA 1, 2, and 3.

For example, the estimated α_t and β_h were obtained from the gradient of slopes shown in Figure 12, for all steps and all directions in the case of TN/2kNm. Here, the blue values (circles) correspond to the left ordinate axis and the red ones (diamonds) to the right one. The coefficients for other transducers were also successfully obtained. All values of α_t and β_h, and their standard uncertainties (standard deviations of the fitting curves) are summarized in Table 4.

All of the comparison calibration results in Figure 10 were corrected by the following equations:

$$\left.\overline{S'_i}\right|_{h40} = \overline{S'_i} - \beta_h\left(h - 40\ \%\right) \text{ and} \tag{2}$$

$$\left.\overline{S'_i}\right|_{t23} = \overline{S'_i} - \alpha_t\left(t - 23\ °C\right) , \tag{3}$$

where h and t are the mean values of the relative humidity and the temperature, respectively, which were measured during torque calibration for obtaining the result $\overline{s'_i}$, and $\left.\overline{S'_i}\right|_{h40}$ and $\left.\overline{S'_i}\right|_{t23}$ are corrected values at relative humidity $h = 40\ \%$ and temperature $t = 23\ °C$ (reference humidity and reference
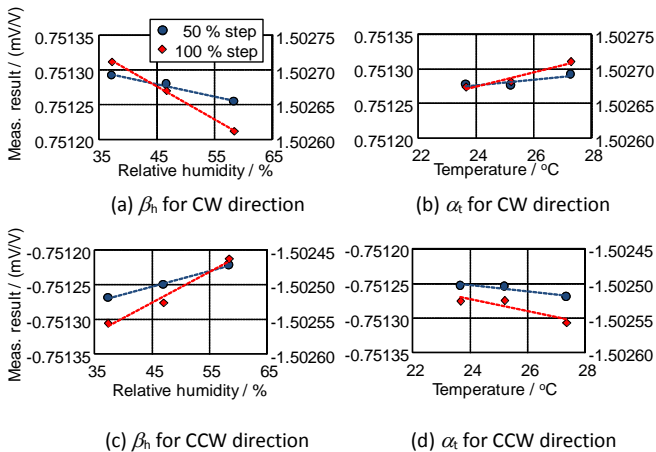
temperature, respectively). In addition, calibration results were corrected by referring the influence of the voltage ratio differences by multiplying correction factors in Table 2.

The calculation results of the short-term drift (with black circles) and the relative deviation (with black squares) between NMIJ and KRISS obtained by using the above corrected values are shown in Figure 10. Almost all relative deviations became smaller than the values without correction. In particular, correction of the humidity achieved good results. On the other hand, short-term drifts did not change much because temperature and humidity conditions were not very different between pre- and post-calibrations at NMIJ.

5.4. Evaluation of E_n numbers

The uncertainties of calibrations including corrections were calculated according to the following equations and procedure. Then, we could finally compare the results of the two NMIs by using the E_n numbers.

5.4.1. Reproducibility with changing mounting position

The relative reproducibility with changing mounting position b was estimated by defining an experimental standard deviation in the measured values for the first measurement loading cycles in all directions, 120°, 240°, 360°, 480°, 600°, and 720°, as follows:

$$b_i = \frac{1}{\left|\overline{S'_i}\right|}\sqrt{\frac{1}{n_{rot} - 1}\sum_{e=1}^{n_{rot}}\left(S'_{i1e} - \overline{S'_i}\right)^2} . \tag{4}$$

The relative standard uncertainty w_{rot} is calculated as "an experimental standard deviation of the mean" by the following equation:

$$w_{rot,i}^2 = \frac{1}{n_{rot}}b_i^2 . \tag{5}$$

5.4.2. Repeatability with unchanged mounting position

The relative repeatability with the unchanged mounting position b' was estimated by defining the experimental standard deviation of the measured values for three measurement loading cycles in the 0° direction as follows:

$$b_i' = \frac{1}{\left|\overline{S'_{i,rep}}\right|}\sqrt{\frac{1}{n_{rep} - 1}\sum_{j=1}^{n_{rep}}\left(S'_{ij0} - \overline{S'_{i,rep}}\right)^2} , \tag{6}$$

where $\overline{S'_{i,rep}}$ is the mean value of the three measured values in the 0° direction (e = 0, n_{rep} = 3).

The relative standard uncertainty w_{rep} is also calculated as "an experimental standard deviation of the mean" by the following equation:

$$w_{rep,i}^2 = \frac{1}{n_{rep}}b_i'^2 . \tag{7}$$

5.4.3. Zero point shift

The relative zero point shift f_0 was estimated by defining the deviation between the zero signals prior to the increasing torque and after the decreasing torque in the first and second cycles of the 0° direction, as follows:

$$f_{0,ij} = \frac{S''_{0j0} - S'_{0j0}}{\left|S'_{nj0}\right|} , \tag{8}$$

(a) β_h for CW direction

(b) α_t for CW direction

(c) β_h for CCW direction

(d) α_t for CCW direction

Figure 12. Estimated temperature and humidity coefficients (TN/2kNm)).

Table 4. Temperature and humidity coefficients for torque transducers and their uncertainties.

Transducer	Torque steps	Temperature coefficient	Standard uncertainty	Humidity coefficient	Standard uncertainty
	N·m	(mV/V)/K	(mV/V)/K	(mV/V)/%	(mV/V)/%
TN/2kNm	1000	4.0.E-06	2.5.E-06	-1.8.E-06	2.7.E-07
	2000	1.0.E-05	2.6.E-06	-4.7.E-06	2.2.E-07
	-1000	-4.6.E-06	1.8.E-06	2.2.E-06	1.3.E-07
	-2000	-8.7.E-06	4.4.E-06	4.4.E-06	6.7.E-07
TB2/1kNm	500	4.8.E-06	1.8.E-06	-1.2.E-07	5.2.E-07
	1000	1.0.E-05	4.1.E-06	-4.3.E-07	1.1.E-06
	-500	-3.2.E-06	5.3.E-07	-5.1.E-07	1.3.E-07
	-1000	-6.0.E-06	1.8.E-06	-1.1.E-06	1.3.E-07
TN/100Nm(MD1)	50	3.3.E-06	3.1.E-06	-2.0.E-06	1.3.E-07
	100	8.0.E-06	2.5.E-06	-5.2.E-06	3.4.E-07
	-50	-4.1.E-06	2.9.E-08	2.2.E-06	1.3.E-07
	-100	-7.3.E-06	2.0.E-06	4.5.E-06	3.7.E-07
TN/100Nm(MD2)	50	-9.0.E-07	3.8.E-07	-3.1.E-06	3.2.E-07
	100	-2.9.E-06	2.0.E-06	-6.8.E-06	5.2.E-07
	-50	3.0.E-06	3.1.E-07	2.8.E-06	9.2.E-07
	-100	4.8.E-06	3.6.E-07	6.3.E-06	1.3.E-06

where i = n is the maximum torque step. The zero point shift cannot be calculated in the last measurement loading cycles because the zero signals after the decreasing torque were read after changing the mounting positions (see Figure 8). The relative standard uncertainty w_{zer} was calculated according to the following equation, considering the mean deviation $f_{0,mean}$ in two $f_{0,j0}$ as the half-width of the rectangular distribution:

$$w_{zer}{}^2 = \frac{1}{3} f_{0,mean}{}^2 . \tag{9}$$

5.4.4. Resolution

In the case of a digital scale, resolution r is defined as one increment in the last active number of the amplifier/indicator when the indication does not fluctuate under the no-load condition. If the indication fluctuates, then r is determined to be half the range of the fluctuation. Here, r is stated in units of torque (N·m).

The uncertainty due to the resolution should be taken into account twice, because each measured value is obtained as the difference between the step-indicated value and the zero-indicated value. The relative standard uncertainty w_{res} was calculated by the following equations for the applied torque T_i (N·m) at step i:

1) Considering the resolution r as the whole width of the rectangular distribution when the indication does not fluctuate under the no-load condition:

$$w_{res,i}{}^2 = \frac{2}{3}\left(\frac{r}{2T_i}\right)^2 . \tag{10a}$$

2) Considering the resolution r as the half-width of the rectangular distribution when the indication fluctuates:

$$w_{res,i}{}^2 = \frac{2}{3}\left(\frac{r}{T_i}\right)^2 . \tag{10b}$$

The low-pass frequency of the amplifier/indicators was always set to "0.1 Hz Bessel" during this bilateral comparison.

In fact, the peak-to-peak fluctuation was only three digits (0.000003 mV/V) in all calibrations.

5.4.5. Short-term drift

The uncertainty due to the short-term drift of the torque transducer during pre- and post-calibrations (J1 and J2) was calculated by the following equation for the increasing torque:

$$w_{dft,i}{}^2 = \frac{1}{3}\left(\frac{\overline{S'_{post,i}} - \overline{S'_{pre,i}}}{2\overline{S'_{J,i}}}\right)^2 , \tag{11}$$

where $\overline{S'_{J,i}}$ is the mean of $\overline{S'_{pre,i}}$ and $\overline{S'_{post,i}}$.

5.4.6. Stability of the amplifier/indicators

The relative standard uncertainty due to the stability of the amplifier/indicators was included as w_{amp} by using the relative standard deviation in Table 2.

5.4.7. Torque by using the TSMs

From the description in Section 2, the relative standard uncertainties of realized torque by using the TSM w_{tsm} are 1.7×10^{-5} for 1-kN·m-DWTSM and 3.4×10^{-5} for 20-kN·m-DWTSM at NMIJ and 2.5×10^{-5} for 2-kN·m-DWTSM at KRISS with a coverage factor of $k = 2$ (equivalent to a confidence level of approximately 95 %).

5.4.8. Influence of temperature and humidity

The standard uncertainties $u(\alpha_t)$ or $u(\beta_h)$ in Table 3 show just the uncertainty of the fitting curves (slopes). The units are (mV/V)/°C or (mV/V)/%. The relative standard uncertainties w_{tmp} and w_{hmd} were calculated by using the following equations:

$$w_{hmd,i} = \frac{u_{hmd,i}}{\overline{S'_i}} = \frac{1}{\overline{S'_i}}\sqrt{u^2(\overline{S'_i}|_{h40}) + \Delta h^2 \cdot u^2(\beta_h) + \beta_h{}^2 \cdot u^2(\Delta h)}$$

and

$$\tag{12}$$

$$w_{tmp,i} = \frac{u_{tmp,i}}{\overline{S'_i}} = \frac{1}{\overline{S'_i}}\sqrt{u^2(\overline{S'_i}|_{t23}) + \Delta t^2 \cdot u^2(\alpha_t) + \alpha_t{}^2 \cdot u^2(\Delta t)} ,$$

$$\tag{13}$$

where Δh and Δt are the relative humidity and temperature deviations from the reference values of 40 % and 23 °C, respectively, $u(\overline{S'_i}\big|_{h40})$ and $u(\overline{S'_i}\big|_{t23})$ are just the measurement uncertainties obtained by the procedure in Section 4.2, and u(Δh) is 1.0 % and $u(\Delta t)$ is 0.05 K.

5.4.9. Evaluation of En number

The relative expanded uncertainty of the calibrations at NMIJ (denoted as the J1 and J2 calibrations) was calculated by the following equation:

$$W_{J,i} = k \cdot w_{c\_J,i} = k \cdot \sqrt{\begin{array}{c} w_{rot,i}{}^2 + w_{rep,i}{}^2 + w_{zer,i}{}^2 + w_{res,i}{}^2 \\ \overline{+ w_{dft,i}{}^2 + w_{tsm}{}^2 + w_{hmd}{}^2 + w_{tmp}{}^2} \end{array}} \ . \quad (14)$$

The relative expanded uncertainty of the calibration at KRISS (denoted as the K calibration) was calculated by the following equation:

$$W_{K,i} = k \cdot w_{c\_K,i} = k \cdot \sqrt{\begin{array}{c} w_{rot,i}{}^2 + w_{rep,i}{}^2 + w_{zer,i}{}^2 + w_{res,i}{}^2 \\ \overline{+ w_{tsm}{}^2 + w_{hmd}{}^2 + w_{tmp}{}^2 + w_{amp}{}^2} \end{array}} \ . \quad (15)$$

The E_n number was also evaluated according to the following equation:

$$E_{n,i} = \frac{\left(\overline{S'_{K,i}} - \overline{S'_{J,i}}\right)/\overline{S'_{J,i}}}{\sqrt{W_{K,i}{}^2 + W_{J,i}{}^2}} \ , \quad (16)$$

where $\overline{S'_{K,i}}$ denotes the result of the calibration at KRISS.

Table 5 summarizes the results of the E_n number evaluation. The relative deviations and the total uncertainties are compared in the results obtained in the two NMIs in Figures 13(a)-13(h). These figures show the relative deviations of KRISS values from NMIJ values. The error bars express the relative expanded uncertainty of measurements obtained from (14) and (15). The E_n numbers were all less than unity in the calibration range from 50 N·m to 2 kN·m. Therefore, the equivalence of the torque standards between NMIJ and KRISS were confirmed.

However, the total measurement uncertainties became much larger than the CMCs of the two NMIs because the uncertainties of the corrections were added; in particular, a somewhat large influence occurred in the results having large differences of the relative humidity. It might arouse much controversy that the more corrections could be considered, the better the result of E_n evaluation becomes, because the total uncertainty necessarily becomes larger than original value (see (16)). As an example of one of solutions for this problem, see the reference [9].

The steps of 500 N·m and 1000 N·m in this comparison coincide with those of CCM.T-K1 (one of the CIPM Key comparisons) [10]. A subject of future study will be to link the comparison results to CCM.T-K1.

6. CONCLUSIONS

An inter-laboratory comparison of the calibrations for torque measuring devices was conducted between NMIJ/AIST and KRISS in the range from 50 N·m to 2 kN·m. Both NMIs have well-established deadweight-type TSMs. In the calibration range from 50 N·m to 2 kN·m, the relative deviations were from 0.2×10^{-5} to 2.4×10^{-5}. Sufficiently small deviations could be obtained between the calibration results of the two laboratories as contrasted with their CMCs, so the equivalence of the torque standards between NMIJ and KRISS was confirmed again. The influences of the stability and difference of voltage ratio spans in the amplifier/indicators as well as the temperature and humidity dependency of the transducer outputs could also be successfully evaluated.

REFERENCES

[1] Y. K. Park, M. S. Kim, J. H. Kim, J. H. Choi and D. I. Kim, "Establishment of torque standards in KRISS of Korea", Proc. 20th Int. Conf. IMEKO TC-3, Merida, 2007, CD-ROM.
[2] M. S. Kim and Y. K. Park, "Design of the 20 kN·m Deadweight Torque Standard Machine", Proc. 22nd Int. Conf. IMEKO TC-3, Cape Town, 2014, USB Flash Drive.

Table 5. E_n evaluation results.

Direction	Torque in N·m	Cal. J in mV/V	Cal. K in mV/V	Rel. Dev. in %	S. T. Drift in %	U_J in %	U_K in %	E_n
TN/2kNm								
CW	1000	0.751265	0.751260	-0.0006	-0.0017	0.0076	0.0064	-0.06
	2000	1.502633	1.502645	0.0008	-0.0013	0.0071	0.0058	0.08
CCW	-1000	-0.751244	-0.751233	-0.0014	-0.0013	0.0075	0.0062	-0.14
	-2000	-1.502522	-1.502508	-0.0010	-0.0036	0.0072	0.0057	-0.10
TB2/1kNm								
CW	500	0.500185	0.500191	0.0012	-0.0009	0.0046	0.0064	0.15
	1000	1.000439	1.000448	0.0008	-0.0008	0.0038	0.0060	0.12
CCW	-500	-0.500193	-0.500182	-0.0021	-0.0011	0.0046	0.0063	-0.27
	-1000	-1.000467	-1.000465	-0.0002	-0.0010	0.0038	0.0057	-0.02
TN/100Nm(MD1)								
CW	50	0.757805	0.757809	0.0006	0.0020	0.0048	0.0064	0.07
	100	1.515693	1.515684	-0.0006	0.0011	0.0040	0.0057	-0.08
CCW	-50	-0.757807	-0.757824	0.0024	-0.0037	0.0049	0.0063	0.29
	-100	-1.515706	-1.515743	0.0024	-0.0042	0.0044	0.0058	0.34
TN/100Nm(MD2)								
CW	50	0.755867	0.755877	0.0013	0.0000	0.0046	0.0067	0.16
	100	1.511800	1.511815	0.0010	-0.0003	0.0039	0.0058	0.15
CCW	-50	-0.755883	-0.755894	0.0015	-0.0008	0.0046	0.0073	0.18
	-100	-1.511855	-1.511872	0.0011	-0.0011	0.0039	0.0062	0.15
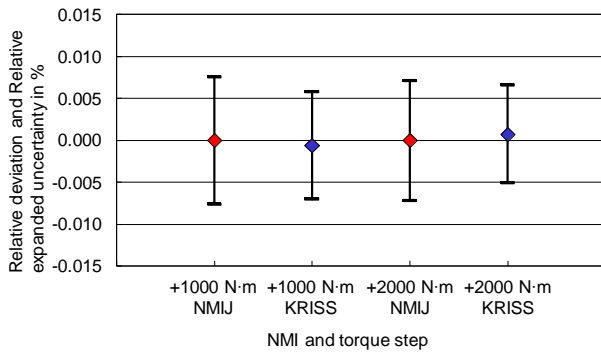
(a) TN/2kNm, CW
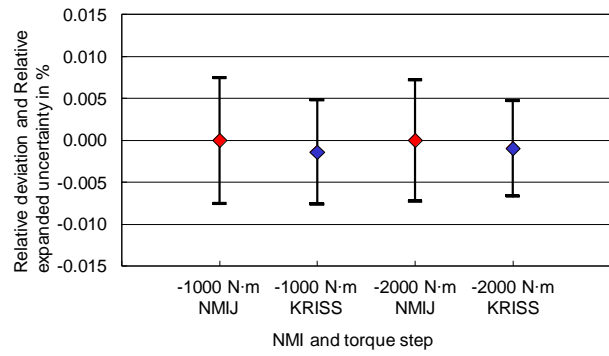
(b) TN/2kNm, CCW
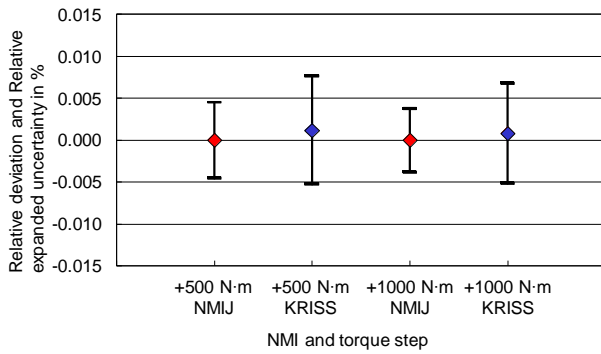
(c) TB2/1kNm, CW
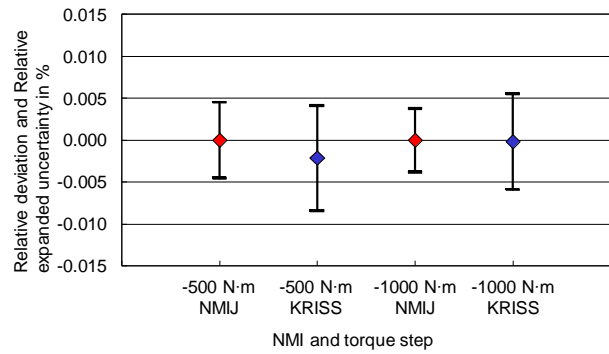
(d) TB2/1kNm, CCW
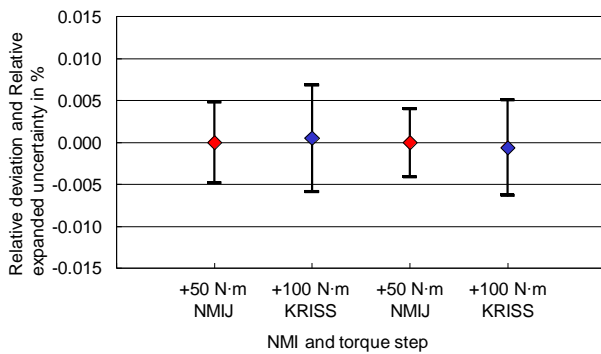
(e) TN/100Nm(MD1), CW
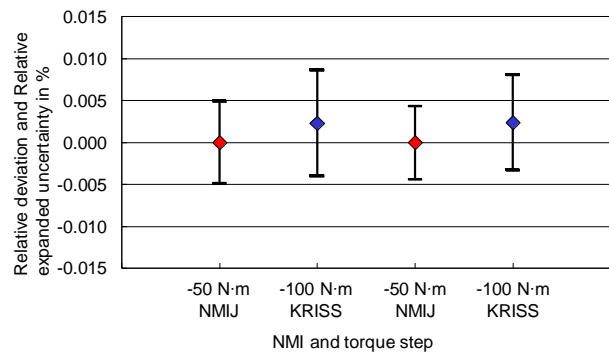
(f) TN/100Nm(MD1), CCW
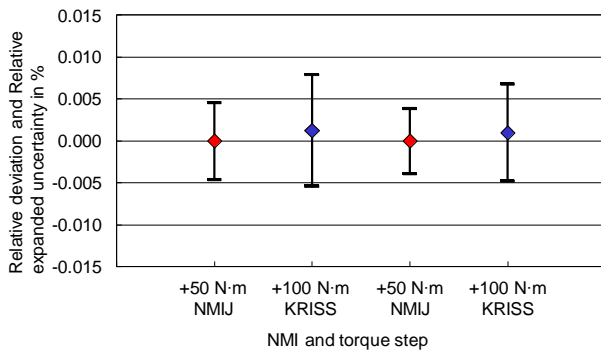
(g) TN/100Nm(MD2), CW
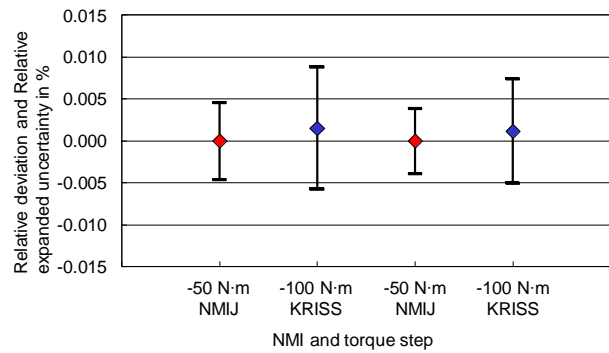
(h) TN/100Nm(MD2), CCW

Figure 13. Relative deviations and uncertainty of comparison calibration.

[3] A. Nishino, K. Ogushi and K. Ueda, "Uncertainty evaluation of a 10N·m dead weight torque standard machine and comparison with a 1 kN·m dead weight torque standard machine", Measurement, 49, pp.77-90, 2014.

[4] K. Ohgushi, T. Tojo and E. Furuta, "Development of the 1 kN·m Torque Standard Machine", Proc. XVI IMEKO World Congress, Vol. 3, Vienna, 2000, pp.217-223.

[5] K. Ohgushi, T. Ota and K. Ueda, "Uncertainty Evaluation of the 20 kN·m Deadweight Torque Standard Machine", Proc. 19th Int. Conf. IMEKO TC-3, Cairo, 2005, CD-ROM.

[6] K. Ohgushi, T. Ota, K. Ueda, Y. K. Park and M. S. Kim, "International Comparison of Torque Standards between the National Metrology Institute of Japan (NMIJ) and Korea Research Institute of Standards and Science (KRISS)", Proc. Asia-Pacific Symposium on Mass, Force and Torque (APMF), Jeju, 2005, CD-ROM.

[7] K. Ohgushi, A. Nishino, T. Ota, K. Ueda, "Expansion of the calibration range and improvement of the uncertainty in the 1 kN·m deadweight torque standard machine", Proc. 20th Int. Conf. IMEKO TC-3, Merida, 2007, CD-ROM.

[8] D. Röske and K. Ogushi, "Final Report on the Torque Key Comparison CCM.T-K2 Measurand Torque: 0 kN·m, 10 kN·m, 20 kN·m", Metrologia, 53, Technical Supplement 07008, 2016.

[9] D. Röske, "A German Torque Comparison from 20 N·m to 200 N·m and Its Results", Proc. 22th Int. Conf. IMEKO TC-3, Cape Town, 2014, http://www.imeko.org/publications/tc3-2014/IMEKO-TC3-2014-015.pdf.

[10] D. Röske, "Final Report on the Torque Key Comparison CCM.T-K1 Measurand Torque: 0 N·m, 500 N·m, 1000 N·m", Internet: http://www.bipm.org/utils/common/pdf/final_reports/M/T-K1/CCM.T-K1.pdf, 2009.